Effects of Extracellular Calcium Depletion on Membrane Topography and Occluding Junctions of Mammary Epithelial Cells in Culture

DOROTHY R. PITELKA, BARBARA N. TAGGART, and SUSAN T. HAMAMOTO
Cancer Research Laboratory and Department of Zoology, University of California, Berkeley, California 94720

ABSTRACT Ca^{2+} dependence of occluding junction structure and permeability, well documented in explanted or cultured epithelial sheets, presumably reflects inherent control mechanisms. As an approach to identification of these mechanisms, we induced disassembly of zonulae occludentes in confluent monolayers of mouse mammary epithelial cells by exposure to low concentrations of the chelators, EGTA or sodium citrate. Stages in disassembly were monitored during treatment by phase-contrast microscopy and prepared for transmission and scanning electron microscopy. Cellular response included several events affecting occluding junctions: (*a*) Centripetal cytoplasmic contraction created tension on junction membranes and displaced intramembrane strands along lines determined by the axis of tension. (*b*) Destabilization of junction position, probably through increased membrane fluidity, augmented tension-induced movement of strands, resulting in fragmentation of the junction belt. (*c*) Active ruffling and retraction of freed peripheral membranes remodeled cell borders to produce many filopodia, distally attached by occluding-junction fragments to neighboring cell membranes. Filopodia generally persisted until mechanically ruptured, when endocytosis of the junction and adhering cytoplasmic bleb ensued. Junction disassembly thus resulted from mechanical tensions generated by initial centripetal contraction and subsequent peripheral cytoskeletal activity, combined with destabilization of the junction's intramembrane strand pattern.

Because they provide the paracellular component of the transepithelial permeability barrier, the zonulae occludentes (occluding or belt tight junctions) of lining and transporting epithelia need to be more stable in position and configuration than many other macromolecular assemblies in the plasma membrane. But structural variations do occur. Remodeling and disassembly of occluding junctions are natural processes during morphogenesis (1–3). In adult epithelia, not only does organization of these junctions differ characteristically among tissues or among cell types within a tissue (4–7), but structural alterations in preexisting junctions may occur during normal physiological transitions, such as cell replacement in the intestine (8) or the onset of lactation in the mammary gland (9). How junction stability and modulation are controlled by the cell, and how structure is related to variations in junction permeability, are matters of continuing speculation (5, 10, 11).

The search for experimental agents that, by inducing nonlethal changes in junction structure or permeability, might provide clues to normal control mechanisms has met with a confounding overabundance of success that has yet to be made sense of. Effective procedures include treatment with proteases (12) or hypertonic solutions (13, 14), mechanical trauma (15), explantation to organ culture (16), and many others. Plant cytokinins cause displacement or proliferation of some junction elements, without interruption in junction continuity, and increase junction tightness as indicated by measurement of transepithelial electrical resistance (17). In contrast, withdrawal of extracellular Ca^{2+} increases junction permeability (18) and leads ultimately to disruption of the junction's morphological continuity (19). Effects of the latter two agents, and of most others tested within physiologically tolerable ranges, are fully reversible.

Freshly dissociated epithelial cells from many organs, and some established cell lines of epithelial origin, can reconstruct in vitro a confluent epithelial sheet in which continuous occluding junctions provide an effective paracellular permeability

THE JOURNAL OF CELL BIOLOGY · VOLUME 96 MARCH 1983 613-624

barrier and polarized transepithelial transport occurs (20–22). Electrophysiological studies of monolayers grown on permeable substrates have demonstrated permeability and transport properties reasonably comparable to the tissues of origin (22–25) and have confirmed the calcium dependence of occluding junctions in culture (26, 27).

In a preliminary study several years ago (28), we observed that occluding junction disassembly in primary cultures of mouse mammary epithelial cells incubated with calcium chelators did not seem to be the passive effect of removal of something that held the cell membranes together, but instead appeared to involve active participation by the cells throughout the process. We therefore chose this culture system for an expanded study of reversible, Ca^{2+}-dependent junction disassembly, our aim being to slow the process enough to identify sequences of morphological events and the relationships between changes in the junctions and in other parts of the cells involved.

In the experiments reported here, we used low concentrations of ethylene glycol-bis (β-aminoethyl ether)-N,N-tetraacetic acid (EGTA) or sodium citrate to chelate extracellular calcium in primary cultures of mouse mammary epithelial cells on plastic or collagen gel substrates. Cellular responses were monitored by phase-contrast microscopy of living monolayers; effects on cell-cell adhesion, junction morphology, and cell topography were determined by electron microscopy. We will show that the events induced by withdrawal of extracellular Ca^{2+} include contraction of the cell body, centripetal migration of microvilli in the apical plasmalemma, destabilization of tight-junction intramembrane organization, elaborate convolution of peripheral membranes in and near the occluding zone, and endocytosis of fragmented tight junctions.

MATERIALS AND METHODS

Cell Culture: Mammary epithelial cells from 3- to 5-month-old BALB/cCrgl mice were dissociated in collagenase, washed, counted, and cultivated in Waymouth's medium with calf serum and hormones as described elsewhere (29). The cells were seeded in plastic 35-mm petri dishes or multiwell plates (well diameter 16 mm), either directly on the plastic or on a layer of hydrated collagen gel, at densities of 5–8 × 10^5 cells/cm^2 on plastic and 1–5 × 10^5 cells/cm^2 on collagen. (Because cell clumps were present and stromal cells were not entirely eliminated, epithelial cell counts are only approximate). Under the culture conditions used, cell proliferation was negligible.

Stock solution of collagen was prepared by dissolving 1 g rat-tail tendons in 250 ml 0.1% acetic acid. Neutralizing solution was 2 parts 10× concentrated Waymouth's medium (without bicarbonate) and 1 part 0.34 N NaOH. 1.5 parts cold neutralizing solution was mixed with 7 parts cold collagen solution and the mixture dispensed quickly, 1.25 ml/35-mm petri dish or 0.3 ml/16-mm well.

Cultures were incubated in a humid environment at 37°C and fed every 2 d. The epithelial pavement was usually confluent by day 4, and most experiments were done at day 5–7 of culture. 1–2 h before the beginning of treatment in many experiments, some of the collagen gels were released from attachment to the plastic dish by loosening the edges with a glass rod and shaking gently. The floating gel and monolayer together then contracted to ~⅔ the original diameter by the time treatment started.

Calcium Chelation: Culture medium was replaced with the appropriate EGTA solution at 37°C (2 ml/35 mm dish and 0.5 ml/microwell); after 1–2 min this was replaced with fresh EGTA solution, and during long incubations of collagen gel cultures the solution was replaced once or twice more. Cultures during treatment were returned to the 37°C incubator or placed on a 37°C warming plate except during observation with a phase-contrast inverted microscope. Solutions used for cultures on collagen ranged from 0.1–1.5 mM EGTA and for those on plastic from 0.6 μM to 1.0 mM; optimal concentrations for slow junction disassembly were 1 mM on collagen and 0.6 μM on plastic, and these were employed in most experiments.

EGTA was dissolved in Ca^{2+}-Mg^{2+}-free Krebs-Ringer bicarbonate buffer or Ca^{2+}-Mg^{2+}-free HEPES-polyvinylpyrrolidone buffer (30) at pH 7.2–8.5. Since increasing alkalinity of the bicarbonate buffer during periods out of the incubator increased the rate of junction disassembly, all later experiments were done with HEPES buffer at pH 7.4 or, for some cultures on collagen, pH 8.0. Mg^{2+} (0.8 mM $MgSO_4 \cdot 7\ H_2O$) was routinely included in the buffer for later experiments, since its exclusion did not detectably affect disassembly.

In some experiments, sodium citrate at 1 mg/ml (on plastic), and 10 or 100 mg/ml (on collagen) in the same HEPES buffer was used as the chelator.

For each set of experimental conditions, some treated cultures were washed and incubated in culture medium overnight to test recovery.

Preparation for Microscopy: Cultures on plastic or on attached collagen gels were fixed in their dishes; floating gels were transferred to vials of the same fixative, 1% paraformaldehyde and 3% glutaraldehyde in 0.075 M sodium cacodylate at room temperature. Subsequent preparation for scanning microscopy and for freeze-fracture and thin-section transmission electron microscopy are described elsewhere (29). 1-μm sections of Epon-embedded specimens were stained with Mallory's methylene blue-Azure II (31) for light microscopy.

RESULTS

Significance of Variations in Experimental Conditions

The variety of conditions described in the preceding section and summarized in Table I was employed for two purposes: to induce gradual, reversible disassembly of tight junctions, permitting identification of steps in the process, and to provide optimal specimens for light-microscope observation during treatment and for thin-section, freeze-fracture, and scanning electron microscopy of treated cultures.

Withdrawal of extracellular calcium induced a centripetal cytoplasmic contraction in a large proportion of cells, accompanied and followed by extraordinary activity of membranes in and around the occluding zone. The interactions of these two processes resulted in a series of changes in cell topography and tight-junction organization that were similar in nature under all of the conditions listed in Table I. The times required for initiation and completion of the series at a given concentration of chelator varied within wide limits, however.

An important experimental variable affecting this timing was the substrate. Our collagen is not highly purified and the gel probably contains other complex molecules, in addition to collagen itself, that are capable of binding Ca^{2+} (32, 33); moreover, its fluid phase consists of Ca^{2+}-containing culture medium. Hence, to obtain comparable effects, much higher

TABLE I

Variations in Experimental Conditions Tested

Substrate	Plastic petri dish or multiwell plate
	Attached collagen gel
	Floating collagen gel
Cell seeding density	On plastic: 3–8 (5*) × 10^5 cells/cm^2
	On collagen: 1–5 (2*) × 10^5 cells/cm^2
Buffer	Krebs-Ringer bicarbonate, Ca^{2+}-Mg^{2+}-free
	HEPES-polyvinylpyrrolidone, Ca^{2+}-Mg^{2+}-free
	HEPES-polyvinylpyrrolidone, Ca^{2+}-free*
Chelating agent, concentration	EGTA (plastic): 0.6 μM*–1.0 mM
	EGTA (collagen): 0.5–1.25 mM (1.0 mM*)
	Sodium citrate (plastic): 1 mg/ml*
	Sodium citrate (collagen): 10*–100 mg/ml
pH	7.2–8.5 (7.4*)
Temperature	22–37°C‡

* Indicates quantity or condition selected for routine use for slow disassembly of junctions.

‡ Average temperature was lower than 37°C because cultures were periodically monitored on an unheated microscope stage.

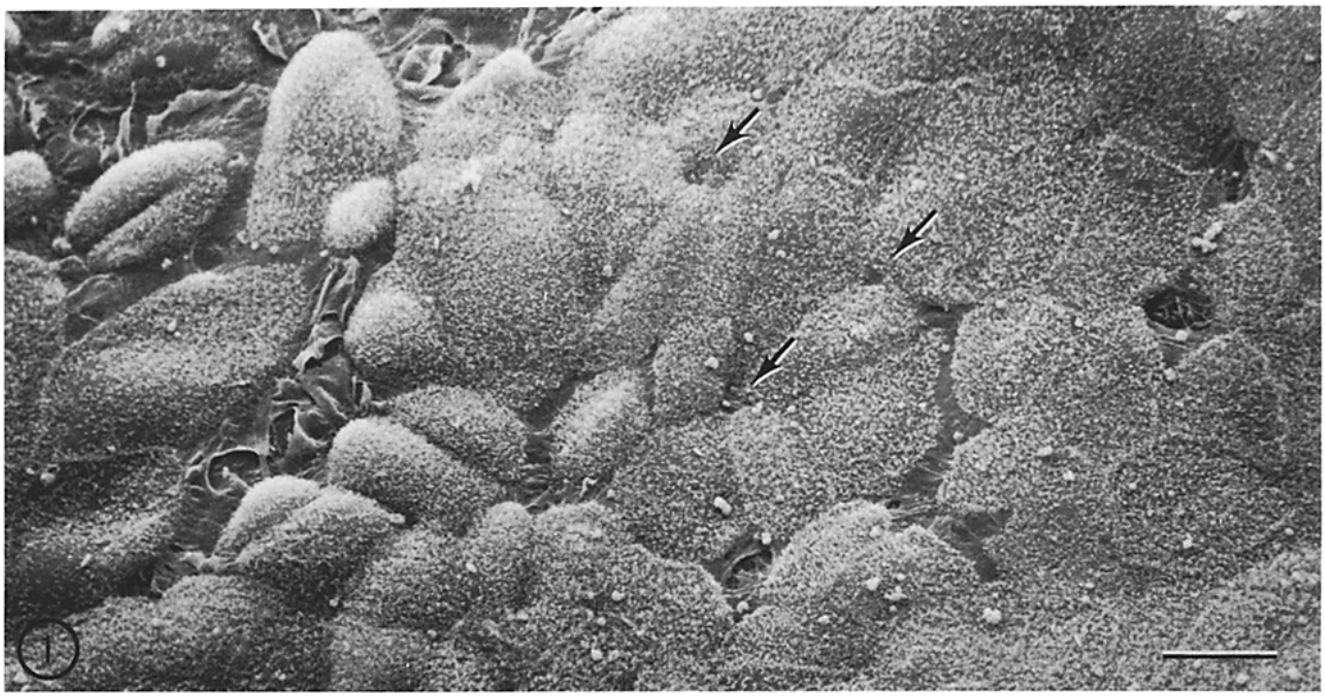

FIGURE 1 EGTA-treated culture on attached gel, illustrating progression of the wave of cellular response from the periphery of the gel (out of field at left) toward the right. Many cells at right and center are not visibly affected; they are flattened, polygonal, and covered with microvilli, and rows of crowded microvilli outline their borders. Other cells show conspicuous clearing of microvilli from cell borders; earliest indications of clearing at three-cell corners are marked by arrows. Left of center, many cells are gently rounded and some show strong contraction, with microvilli crowded on the apical bulge. Gaps in continuity of membrane contact between cells have appeared in several places, and ruffling of freed membranes is evident. 0.75 mM EGTA, 3 h. Bar, 20 μm. × 1,500.

concentrations of chelating agents were required for cultures on gel than those on plastic. On attached gel, where the epithelial pavement constitutes a permeability barrier to diffusion of the chelator into the gel, cellular response always began at the periphery of the gel, or around any chance or deliberately created discontinuities in the cell sheet, and spread slowly from these sites (Fig. 1). A similar but always faster progression of effects from the periphery or from gaps in the epithelial layer was observed in cultures on plastic. Cells on floating gels showed less variation in reaction time than those on attached gels, but were not synchronous.

Within the ranges indicated in Table I, higher concentrations of chelating agents, higher temperatures, and higher pH all tended to hasten response in any given experiment, without appreciably altering its course. Since the gamut from apparently unaffected cells to almost complete cell separation could be observed within single cultures (Fig. 1), it is not possible to stipulate average response times for any treatment. For these reasons, it will be evident that data on chelator concentration and exposure time, reported in figure legends, are not consistently related to extent of cellular response. The essentially similar course of events in this response under all the conditions employed, however, suggests that we are observing a pattern of basic cellular mechanisms.

Morphology of Control Cultures

As described elsewhere (21, 29, 34), prelactating mammary cells on either plastic or collagen substrates form typical epithelial pavements of polygonal cells bearing apical microvilli and joined by occluding junctions. Cells on plastic flatten and spread broadly and, whatever their density at confluence, overlap extensively; where a peripheral lamella of one flattened cell overlaps another, the occluding junction membranes lie in approximately the same plane as the overlapped cell's apical surface (Fig. 2). Cell spreading on collagen is less extreme, and peripheral overlap is less extensive; occluding junction membranes usually are gently curving or approximately perpendicular to the apical surface (Figs. 3 and 4), rarely parallel to it. Lateral membranes below the apical junctions are variably contorted.

Intramembrane strands of mammary occluding junctions in culture typically are undulatory, like those of the gland in situ (9), and continuous strands are likely to be roughly parallel to the single strand that forms the junction's apical border (Fig. 2).

Morphological Events in Ca^{2+}-dependent Junction Disassembly

CLEARING OF PERIPHERAL MICROVILLI AND CYTOPLASMIC CONTRACTION: An early effect of Ca^{2+} chelation observed by scanning microscopy is the clearing of microvilli from one or both sides of a border between cells, usually beginning at the corners where three cells meet (Fig. 1). The onset of microvillar clearing is soon followed by visible contraction of cell bodies (Figs. 1 and 5), eventually producing a rounded central hump covered by abnormally crowded microvilli. As is evident in Fig. 1, variability in rate and extent of response by neighboring cells, or by sectors of one cell's circumference, prevails throughout the course of junction disassembly.

The continuity of contact between cells in treated cultures initially is maintained, while their borderlines become minutely and irregularly contorted (Fig. 6). That this distortion is three-

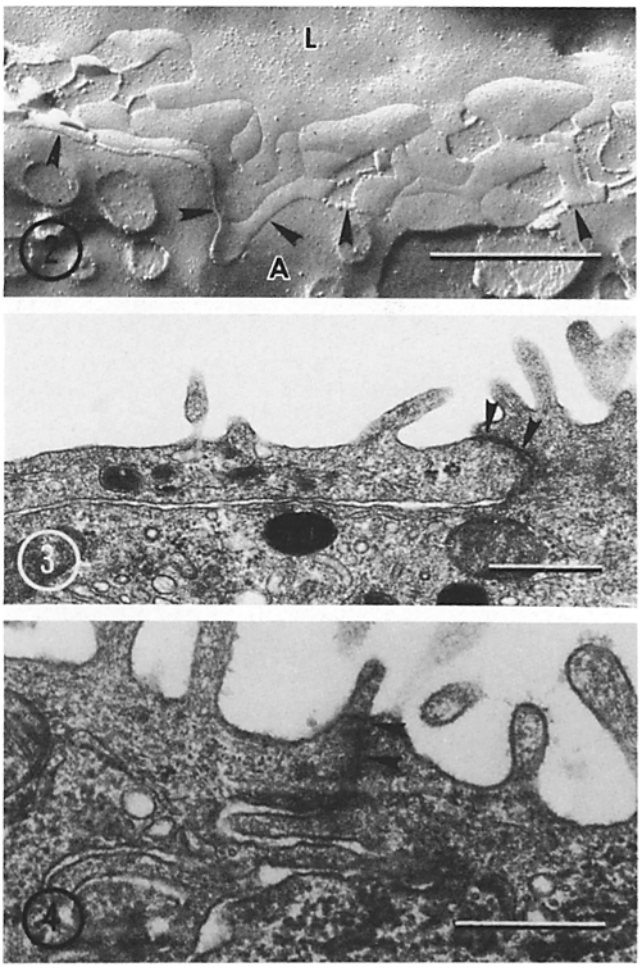

FIGURES 2–4 FIGURE 2 Freeze-fracture replica of a typical occluding junction in cell culture. In this control monolayer on plastic, lateral (*L*), junctional, and apical (*A*, with fractured bases of microvilli) membranes lie in the same plane, indicating overlap. Most of the junction is seen as a network of furrows on the exoplasmic face of the overlapping cell's membrane. At the apical border strand (arrowheads) of the junction belt, and in several spots within the junction, the fracture plane shifts to the protoplasmic face of the underlying cell's membrane. The course of the apical border strand is relatively straight, except for one abrupt curve onto the apical membrane, approximately paralleled by the next subapical strand. Bar, 0.5 μm. × 45,000. FIGURES 3 and 4 Vertically sectioned apical junction zones in control cells on collagen gels. Approximate limits of occluding junctions are indicated by arrowheads; below them in both figures are shallow adhaerens junctions. Fig. 3 is an example of peripheral overlap, with a shallow, curving, junction zone. Bar, 0.5 μm. × 30,000. In Fig. 4, a vertical junction complex is followed by interdigitating processes, representative of the variable contours of laterobasal membranes in culture. Bar, 0.5 μm. × 40,000.

dimensional, affecting junctional membranes below their apical borders, is often evident in thin sections (Fig. 7). We report elsewhere (29) that extraordinary centripetal tension, created by EGTA-induced contraction or by the extreme spreading of untreated cells in low-density monolayers on plastic, may lead to exaggerated sinuosity of the continuous apical border strand of the occluding junction, which defines the borderline between the two cells. In areas of peripheral overlap, tension may lead further to an alignment of subapical strands roughly perpendicular to the overall direction of the border and presumably parallel to the axis of tension (Fig. 8 and reference 29). This alignment represents an equilibrium condition in untreated cultures, but progressive changes ensue in the presence of calcium chelators.

DESTABILIZATION OF OCCLUDING JUNCTIONS AND PERIPHERAL MEMBRANE ACTIVITY: Whereas the alignment of junction strands induced by sustained tension alone usually does not entail significant interruption in continuity of the apical border strand, such discontinuities do appear in EGTA- and citrate-treated cultures. In Fig. 9, the membranes in an area of overlap are relatively flat, microvillar clearing has begun, and strand realignment is pronounced. In addition to realignment within the original junction zone, two single strands and a multistrand cluster extend from its apical edge into the apical membrane, terminating at the bases of microvilli or other surface processes. The apical edge of the junction is angular and deeply dissected, no longer defined by a single, undulating border strand.

Further distortions of junction organization become evident as clearing of microvilli proceeds. Both sides of the borderline between two cells shown in Fig. 10 are cleared for a distance of a micrometer or more. Single or narrowly looped strands from the junction are drawn out in the apical membranes of both cells, ending without association with surface protrusions.

An alternate arrangement sometimes is seen where parallel cell membranes are flat over a relatively large area. In Fig. 11, junction elements are distributed in parallel rows of disconnected single or clustered strands. Their alignment suggests the combined influences of tension and destabilization in an exceptionally broad zone of peripheral overlap, and their number and aggregate length suggest that they may represent a large proportion of strands from a nearby junction. Unlike the instances in Figs. 9 and 10, many small macular junctions, unconnected with any junction belt, have formed.

These altered strand configurations were seen in areas where the joined membranes remained relatively flat and the paired membranes of each junction were maintained in good contact; in section, cells in such areas probably would resemble those in the left half of Fig. 5*b*. Scanning micrographs reveal that the peripheral membranes soon develop ridges or ruffles, and gaps begin to appear in the continuity of cell contact (Figs. 1,

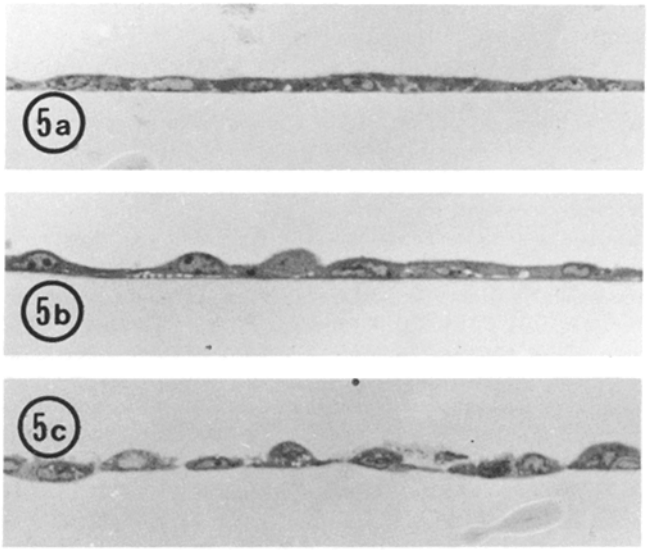

FIGURE 5 Photomicrographs of 1-μm sections of cells on attached gels, illustrating shape change during EGTA treatment. (*a*) Untreated control monolayer of low cuboidal cells. (*b*) 1 mM EGTA, 54 min. (*c*) 1 mM EGTA, 75 min. × 560.

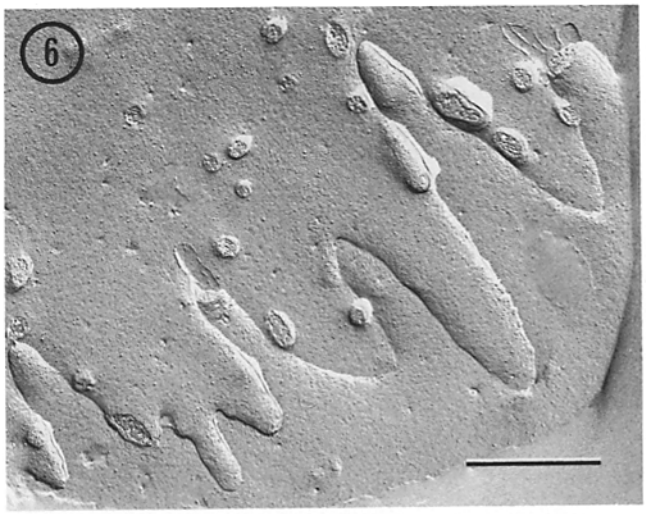

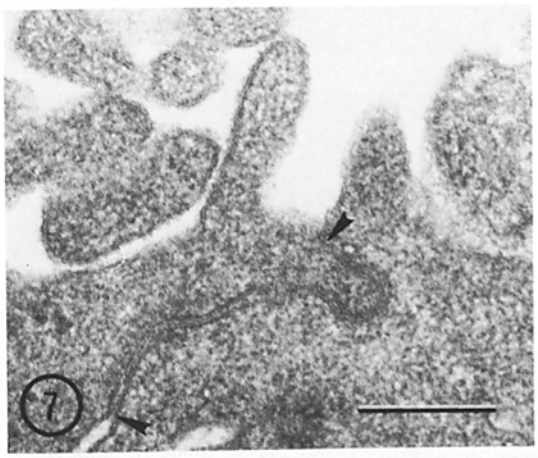

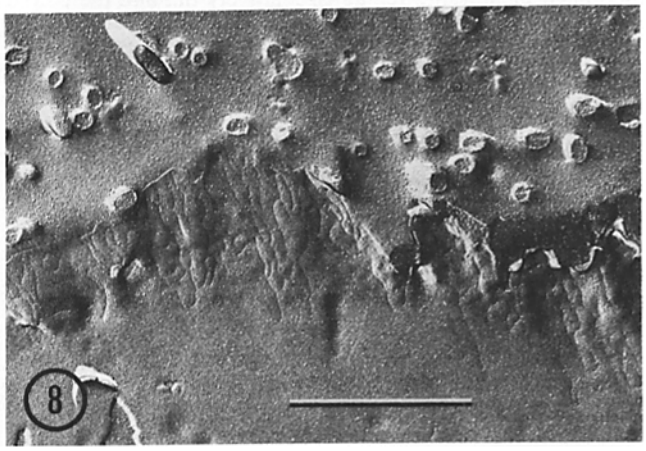

FIGURES 6–8 FIGURE 6 Replica of intact, convoluted borderline between cells on plastic. Fractured bases of microvilli appear at the border of the cell in upper left but are absent from the cell at lower right, suggesting that clearing of microvilli from the latter's border had begun. The tips of two overlapping fingers from the lower cell are fractured away, revealing convolution of the junction's apical border strand. 0.6 μM EGTA, 6 min. Bar, 0.5 μm, × 35,000. FIGURE 7 Section cut perpendicular to the plane of a monolayer on collagen gel. Apical and basal limits of occluding junction profile are indicated by arrowheads. Although border microvilli of both cells are still in place, junctional membranes are contorted. 0.5 mM EGTA, 10 min. Bar, 0.2 μm. × 90,000. FIGURE 8 Occluding junction in area of overlap in culture on plastic. Sinuosity of apical border strand and perpendicular orientation of subapical strands (seen here as E-face furrows) are similar to those in untreated low-density cultures. Fractured bases of microvilli on adjacent apical membrane show that clearing had not begun. 0.6 μM EGTA, 3 min. Bar, 1 μm. × 24,000.

12). Numerous filopodial processes develop, extending from the edge of one cell toward the microvillar island on the neighboring cell or from one microvillar island to the other. Processes from each cell initially lie on the surface of its neighbors' peripheral membrane and, in at least some cases, are attached to it by tight junctions consisting of one or a few long strands (Fig. 13). These observations indicate that the strands extending from the junction belt into the apical surface membranes in Figs. 9 and 10 also were sites of attachment of recumbent filopodial extensions from the companion cell. Where the origin of a filopodium and its termination on the partner cell's surface are not obscured by microvilli or other structures, it often appears in scanning micrographs that the distal end of the process is embedded in an indentation of the surface membrane (Fig. 14).

The extent of membrane activity often observed as events proceed is strikingly demonstrated in scanning micrographs (Fig. 15) and in thin sections cut perpendicular to the culture plane (Fig. 16). Between contracted cells are multilayered, interdigitating or extravagantly contorted, lamellar and filopodial processes. Most of these originate in a band 1–4 μm wide, which circumscribes the base of the apical bulge and may involve more than just the area formerly occupied by the zonula occludens.

Occasional cells in any treated culture remain in close lateral contact during EGTA-induced contraction, displaying neither unusual membrane contortions nor evidence of tension. In some of these, destabilization of junction organization is nonetheless indicated by atypical strand arrays. In some instances, junction continuity is disrupted by apparently random displacement of strands. In others, a continuous apical junction belt of variable depth persists, but additional strands extend in unpatterned arrays far down the lateral cell membranes, a phenomenon reported for other cell types and experimental conditions (35).

MEMBRANE RETRACTION AND ENDOCYTOSIS OF TIGHT-JUNCTION FRAGMENTS: Figs. 1, 12, and 14–15 show that gaps in the continuity of occluding junctions increase in number and size with continued absence of extracellular Ca^{2+}, and that the initially short spans of peripheral membranes thus freed from attachment to neighboring cells usually become convoluted. In time, most of the freed membranes retract toward the cell body, leaving behind elongated lamellar or filopodial processes still attached by isolated tight junctions. Eventually, the majority of cells retain direct contact with their neighbors only through such processes (Fig. 17). Fig. 5*c* illustrates the profile of a monolayer at or near this stage.

Contorted membrane topography prohibits freeze-fracture analysis of junction fragmentation and disassembly during these events. However, the distal attachment of a slender process by a tight junction, usually in an indentation of the partner cell's surface, is often identifiable in thin sections. Figs. 18–20 illustrate a range of structures very frequently observed. Fig. 18 shows the insertion of an intact filo- or lamellipodium. In Figs. 19 and 20, small, membrane-limited structures lie in surface depressions to which they are attached by tight junctions. These could be either the ends of intact processes not otherwise included in the plane of section or blebs left by rupture of a process proximal to its insertion on the neighboring cell. Figs. 21 and 22 may represent stages in endocytosis of

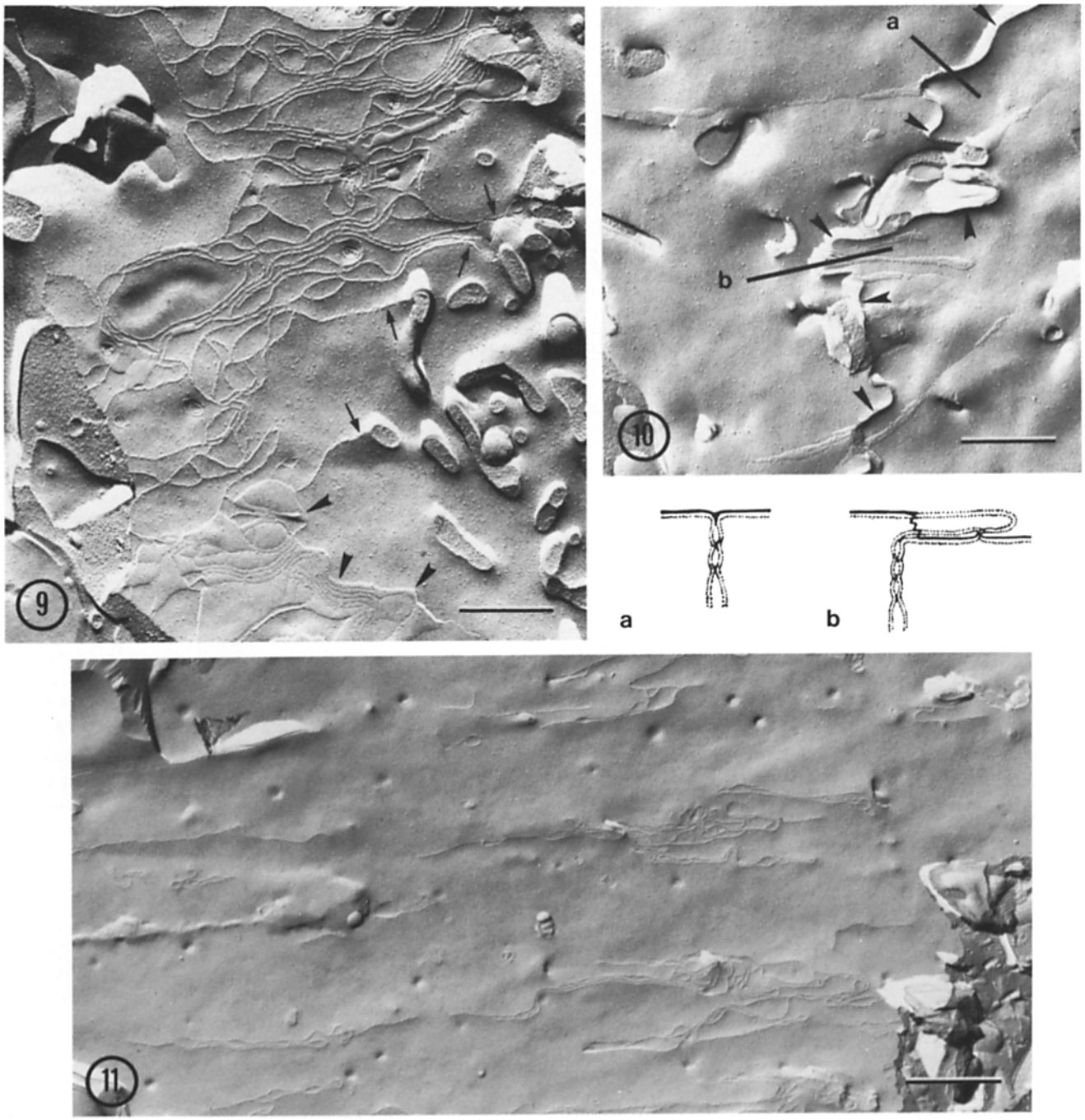

FIGURES 9–11 FIGURE 9 Occluding junction in area of overlap in culture on plastic. The P face of the apical surface membrane of the overlapped cell is seen at right, with fractured microvillar bases (two or more microvilli often arise from a common elongate base). Virtually all strands are roughly perpendicular to the overall course of the junction belt; the original apical border strand is not identifiable except for a short distance at the bottom of the field (arrowheads). Arrows point to strands that extend from the junction across a microvillus-free apical area to terminate at the bases of microvilli. 1 mg/ml sodium citrate, 15 min. Bar, 0.5 μm. × 30,000. FIGURE 10 Replica of a sinuous borderline (arrowheads) between two cells, and microvillus-free peripheral membranes on either side. Subapical membranes of the junction belt have been fractured away, leaving parts of its apical borderline represented by intact segments of a curving, sharp ridge. Elongate tight-junction grooves extending from the borderline show that slender fingers from each cell's border overlapped the peripheral membranes of the other. Culture on plastic, 1 mg/ml sodium citrate, 15 min. Bar, 0.5 μm. × 30,000. *a* and *b* are sketches of membranes at lines *a* and *b* as they would appear in section perpendicular to the page. Solid lines represent the exoplasmic leaflets visible in the replica. Dotted lines represent projections of adjacent membrane elements lying behind or in front of the replica. FIGURE 11 Part of a large (about 75 μm^2) membrane fracture face containing an array of discontinuous parallel rows of aligned tight-junction strands. Culture on plastic, 0.1 mM EGTA, 14 min. Bar, 1 μm. × 15,000.

tight junction patches with remnants of the attached process, as reported in other tissues (36–40).

Cultures on plastic and on floating collagen gel at or near the endpoint of changes in topography induced by Ca^{2+} chelation are compared in Figs. 23 and 24. In Fig. 24, most cells, originally broadly spread, are moderately to strongly con-

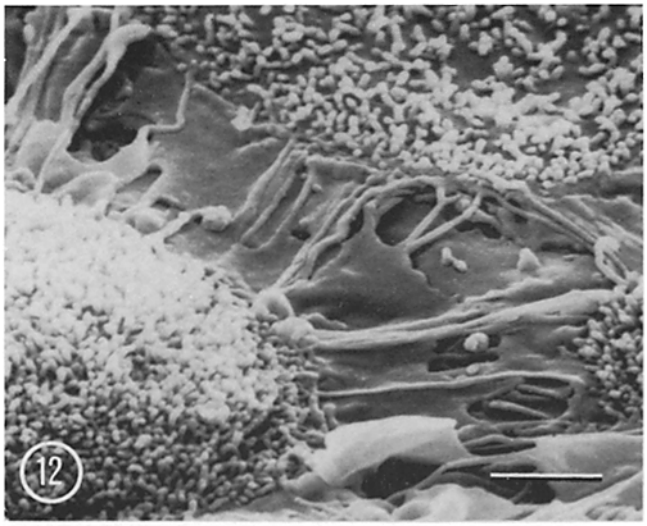

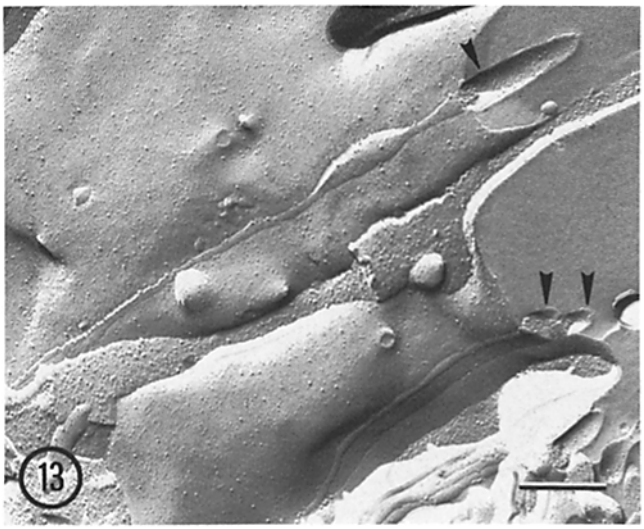

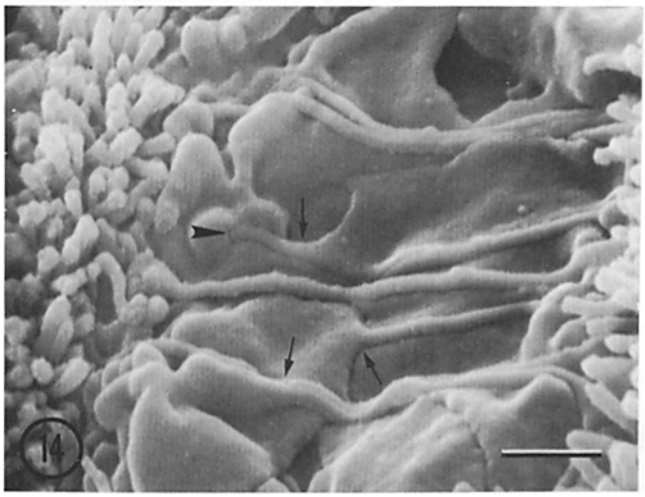

FIGURES 12–14 FIGURE 12 Peripheral membrane activity after clearing of microvilli in a culture on collagen. Continuity of membrane contact at borderlines between cells is repeatedly interrupted, and freed membranes often are ruffled. Many filopodia extend from the periphery of each cell to the microvillus thicket of its neighbor; most are recumbent on the neighbor's membrane, but some clearly are free. 1.0 mM EGTA, 40 min. Bar, 1 μm. × 7,500. FIGURE 13 Tight-junction attachment of filopodia to peripheral membrane of another cell. The exoplasmic leaflet of the membrane occupies most of the figure and is traversed from middle left to upper right by a pair of junction furrows. At upper right, the fracture plane leaves the membrane, passing obliquely through the recumbent filopodium (upper arrowhead) that was attached by this junction. At lower right are two additional, cross-fractured filopodia (lower arrowheads); furrows of their tight junctions are just visible in a membrane valley extending toward lower center. 0.6 μM EGTA, 1.5 h. Bar, 0.25 μm. × 45,000. FIGURE 14 Filopodia lying on distorted peripheral membranes in culture on gel. Origins (arrows) of several filopodia from membrane borders are visible; their distal ends are obscured by microvilli or other filopodia, except for one that inserts in the companion cell's surface (arrowhead). 1 mM EGTA, 40 min. Bar, 0.5 μm. × 26,000.

tracted and are connected to each other and to the substrate by long, taut filopodia or lamellar extensions. Epithelial monolayers on floating gels are initially less broadly spread, and also have spontaneously contracted to some extent before the chelator is added. Although the cytoplasmic contraction induced by calcium chelation could in theory be accommodated by further contraction of the cells and gel without disruption of intercellular junctions, this does not happen (Fig. 24). Strong apical contraction takes place, and peripheral membranes become as contorted as they do on attached gel (Fig. 17) or plastic; the cells on floating gels are closer together, however, and filopodia at the endpoint tend to be fewer and shorter.

In the absence of mechanical agitation, this state may persist through the longest treatment periods used in our experiments—up to 3 h. However, mild mechanical stress, such as swirling of the bathing solution incidental to handling of culture vessels, and probably the surface movements of the cells themselves, can result in rupture of intercellular filopodia, leaving disembodied distal ends to be disposed of by endocytosis. Rupture or withdrawal of substrate attachments often follows in cultures on plastic, yielding a suspension of single or clustered cells. Cells on collagen usually remain attached to it throughout treatment and will reestablish a confluent monolayer if washed and allowed to recover in culture medium. A companion to the culture in Fig. 24, exposed to 1 mM EGTA at pH 8 for 2.5 h, had recovered after 4 h to the condition shown in Fig. 25; by 24 h of recovery, another sister culture was indistinguishable from untreated controls.

DISCUSSION

We have employed three different ultrastructural techniques to observe changes in cell topography, intercellular relationships, and occluding junction morphology induced in cultured epithelial monolayers by chelation of extracellular calcium. The accumulated evidence permits us to attempt a reconstruction of the probable sequence of and interactions among events described by these methods.

Junction Disassembly

The initiating event appears to be the Ca^{2+}-dependent development or enhancement of centripetal contractile tension in the cytoskeleton, with immediate effects on peripheral membranes preceding visible rounding of the apical cell surface. Distortion of junction membranes is evident as exaggerated sinuosity of apical borderlines between cells, and often as convolution of the subapical profiles of joined membranes in vertical section. Where the junction between a flattened cell

and an overlapping peripheral lamella of its neighbor is subject to opposing tensions in the two cells, a frequent effect is the alignment of subapical strands roughly perpendicular to the axis of the junction and parallel to the prevailing axis of stress. We suggest that such axes are created in the cortical cytoskeletal meshwork, which in turn is linked by unknown connectors to the junction's intramembrane strands (29).

While these changes in junctional membranes are going on, clearing of microvilli from the cell borders begins. Clearing could result from reabsorption of microvilli into the apical membrane or from centripetal migration in a fluid membrane. Short, stubby microvilli, which might be stages in growth or resorption, usually are evident in scanning micrographs of partially cleared borders, but they are also common in untreated control cells. Evidence of centripetal migration is provided by the extraordinarily high density of microvilli on the apical hump at maximum contraction and by the presence of tight-junction strands extending from the apical edge of a junction across the cleared apical membrane to the bases of microvilli. The latter phenomenon suggests that the microfilament core of a border microvillus and the cytoskeletal linkage to a contiguous junction strand (necessarily the apical strand, perhaps with one or more connecting subapical ones) have been entrained together in the centripetal contraction. Since each strand being displaced is physically paired with its twin in the partner cell's membrane, that membrane is dragged along in the form of an overlying filopodial extension. In this way, the borders of both cells may be drawn out as interdigitating, overlapping processes.

Microvillar clearing was not observed in cells subject to mechanical tension only (29). It follows that chelation of external Ca^{2+} is responsible for the increased mobility of intramembrane and membrane-linked structures (41, 42). This may in time result in loss of continuity of the apical strand of the occluding junction, on which the other strands are inserted, and create strand-free pathways across the junction belt. Destabilization of junction configuration in the absence of extracellular Ca^{2+} is further manifest in the apparently random disarray of strands in some areas displaying no effects of tension.

Gaps in continuity of the junction belt allow the disjoined membranes to separate locally. The ensuing ruffling and retraction of freed membranes would be expected to create new, local tensions resulting in further fragmentation and migration of occluding junctions and freeing of more peripheral membrane. Eventually, most of the once-continuous belts are reduced to patches attaching filopodial or lamellar processes distally to the neighboring cell's surface.

Many of these patches are removed by endocytosis soon after they are formed. We do not know whether endocytosis occurs only after rupture of the connecting cytoplasmic extension, or may sometimes be a kind of gentle cannibalism, one

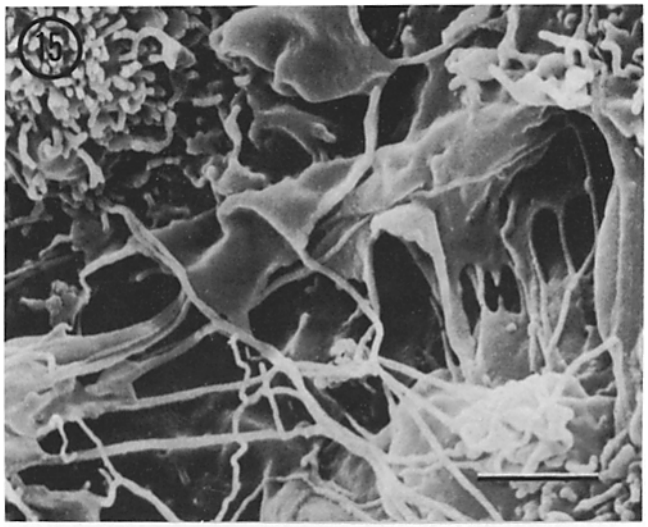

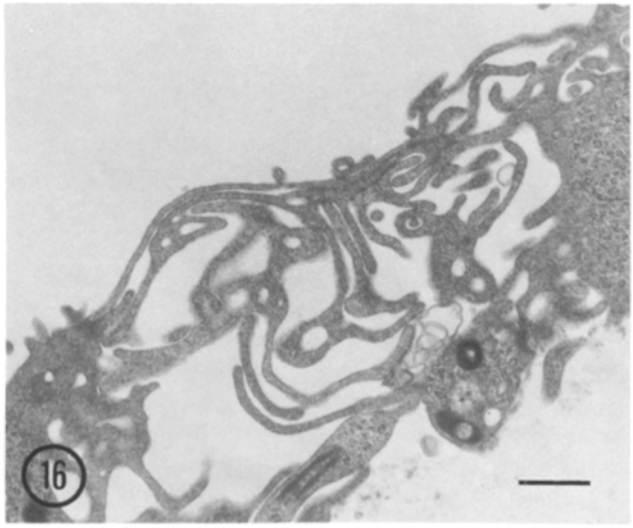

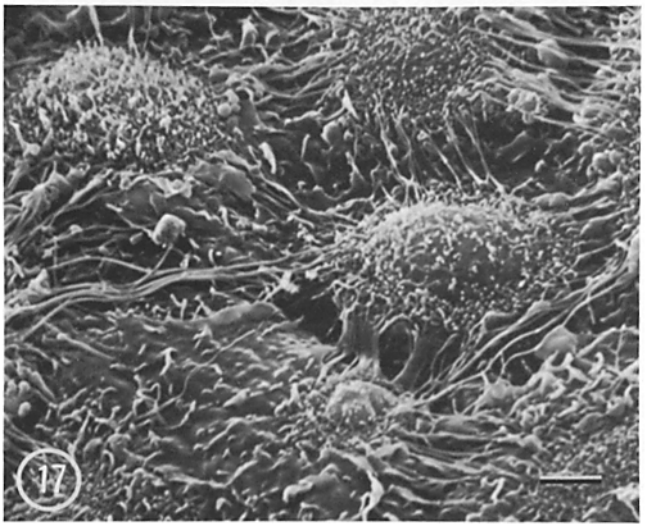

FIGURES 15–17 FIGURE 15 Peripheral membrane ruffling and retraction in culture on gel. Membrane borders have withdrawn, leaving unsupported long filopodia crossing the intercellular space. The view is downward into the space between three cells; it is evident that lamellar membranes and filopodia are present at various levels below the original apical surface. 0.75 mM EGTA, 35 min. Bar, 2 μm. × 8,000. FIGURE 16 Peripheral membranes of two cells on gel, sectioned perpendicular to culture plane, at a stage like that illustrated in Fig. 15. The elaborately interdigitating processes include slender filopodia and lamellipodia of unknown width, often branched or perforated. The thinner processes are the diameter of a microvillus or less. 1 mM EGTA, 60 min. Bar, 0.5 μm. × 19,000. FIGURE 17 Most of the cells in this field from a culture on gel are contracted and are directly connected to neighbors by fine filopodia. Their remaining peripheral membranes show frequent ruffling. 1 mM EGTA, 53 min. Bar, 2 μm. × 4,000.

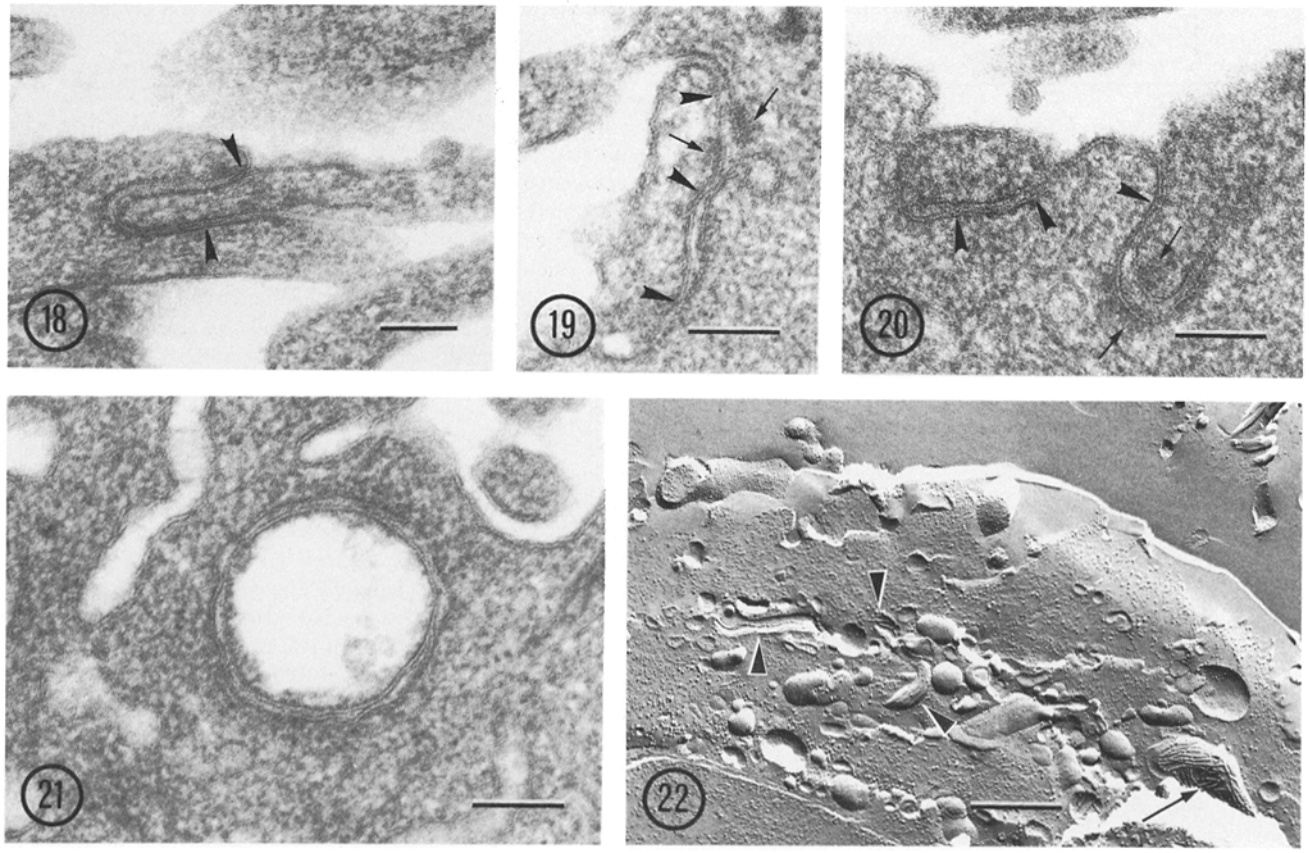

FIGURES 18–22 FIGURE 18 A blunt extension from the surface of the cell at left contains a U-shaped depression, within which the tip of a slender process (which was traced beyond this field to its origin from a neighboring cell) is attached by a tight junction. Arrowheads indicate identifiable points of fusion of membrane outer leaflets. 1 mM EGTA, 60 min. Bar, 0.1 μm. × 100,000. FIGURE 19 A flat process or cellular fragment is attached to a shallow depression in a cell surface. Arrowheads indicate apparent tight-junction fusions. Two slightly offset submembrane densities (arrows) resemble a distorted small desmosome, suggesting that these joined membranes are a remnant of the original junctional complex. 1 mM EGTA at pH 8, 20 min. Bar, 0.1 μm. × 120,000. FIGURE 20 Tips of two processes insert in a cell surface. Membrane fusions are indicated by arrowheads. Submembrane densities (arrows) in the right-hand structure again suggest persistence of desmosome elements adjacent to a tight-junction patch. 1 mM EGTA at pH 8, 20 min. Bar, 0.1 μm. × 120,000. FIGURE 21 Possible stage in endocytosis of tight-junction remnant. The vesicle is near the cell surface and could still have been in continuity with a persisting cytoplasmic process. However, loss of most of the enclosed cytoplasm suggests rupture of nearby membrane. Plasmalemma of the visible fragment is intact and clearly attached by tight-junction fusions to the vesicle membrane of the host cell. 1 mM EGTA at pH 8, 20 min. Bar, 0.1 μm. × 120,000. FIGURE 22 Replica of paranuclear cytoplasm in a cell on collagen. Long arrow at right points to a large endocytic vesicle; the P-face junction strands are those in the membrane of the enclosed fragment. Arrow heads point to slender, elongate endocytic vesicles displaying tight-junction strands in the vesicle membrane. 1 mM EGTA, 52 min. Bar, 0.5 μm. × 24,000.

cell pinching off the tip of its neighbor's intact extension by closure of a vacuole around it. The latter may be facilitated by the typical distal insertion of filopodia in depressions of the cell surface.

Because most mammary cells on collagen retain their attachment to it in the presence of Ca^{2+} chelators, a large proportion of tight-junction patches in our cultures remain intact and in place as long as connecting filopodia are not mechanically ruptured.

Another putative mechanism for opening of junctions is lateral dispersion of constituent intramembrane particles, accompanied by disruption of whatever bonds hold the paired elements in the two membranes together. We have seen no evidence of this process, which is suggested for tight or gap junctions in some other cells (3, 39, 43, 44); by its nature it is difficult either to prove conclusively or to disprove.

The essence of our observation is that the fragmentation of occluding junctions induced in mammary epithelial monolayers by withdrawal of extracellular Ca^{2+} results from increased cytoskeletal activity combined with enhanced mobility of intramembrane elements of the junction. Cell separation requires mechanical disturbance in addition.

Calcium Chelation and Cell Contraction

The contractile response of mammary cells to extracellular Ca^{2+} chelation is very like that described by Britch and Allen (45) in a normal rat liver (NRL) cell line treated with 21 mM EGTA. In their whole-cell transmission electron micrographs, a peripheral ring of microfilaments was evident, the contraction of which herded cytoplasmic organelles toward the bulging cell center. Thin peripheral lamellae remained attached to the substrate, but became fimbriated and ultimately converted to long, branching retraction fibers radiating from the rounded cell body. Similar contractile response to Ca^{2+} or Ca^{2+}-Mg^{2+} withdrawal, without loss of substrate attachment, is reported for other cell types, including 3T3 fibroblasts (46), lens epithelium (47), and ovarian granulosa cells (48). Cytoskeletal retrac-

tion from cell peripheries was also demonstrated (49) in EGTA-treated canine kidney cell (MDCK) monolayers by immunofluorescent labelling of either actin or tubulin. The effects of withdrawal of extracellular Ca^{2+} on intracellular Ca^{2+} levels in these cases is unknown, and the mechanism of induction of cytoplasmic contraction is unexplained.

Calcium and Occluding Junction Stability

Sedar and Forte (18) showed in 1964 that treatment of frog stomach with 1–4 mM EDTA (ethylenediaminetetraacetic acid, which chelates both Ca^{2+} and Mg^{2+}), in addition to increasing transepithelial permeability, caused separation of adhaerens junctions and distortion or blistering of occluding junction membranes. More recently, protocols developed for high-yield dissociation of epithelial tissues typically have included exposure to Ca^{2+}-free solutions, with or without a chelator, with collagenase or as a separate step after protease treatment, and accompanied or followed by mechanical agitation (e.g., references 50, 51). Berry and Friend (50) first identified tight-junction patches attaching membrane blebs to the surfaces of dissociated cells and concluded that, after opening of adhaerens junctions by chemical treatment, tight (and gap) junctions were mechanically torn out of the membrane of one of the joined cells. Such blebs have since been seen in recently dissociated cells by others (39, 51, 52). Reduction of junction belts to patches as an effect of Ca^{2+} withdrawal results in smaller membrane wounds during tearing, probably improving cell viability.

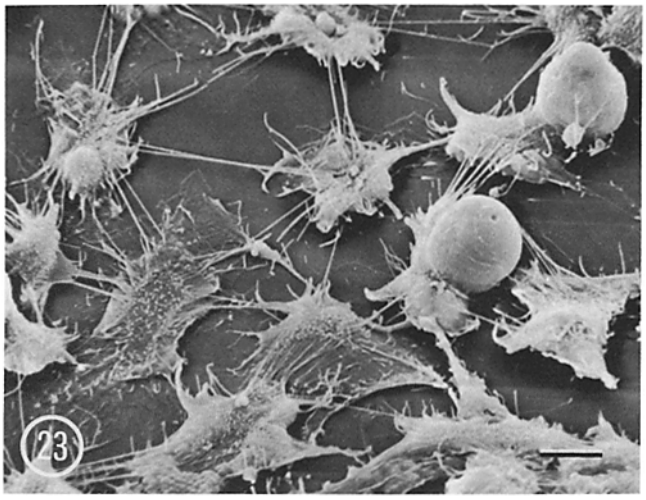

FIGURE 23 Culture on plastic. Most cells are rounded or bluntly stellate and are interconnected by filopodia, some of which were broken during processing for microscopy. Attachment to the substrate by slender or lamellar extensions is maintained in most areas. 0.5 mM EGTA, pH 8.4, 6 min. Bar, 5 μm. × 1,600.

In the most extensive previous studies of effects of EGTA at relatively low concentrations on the structure of occluding junctions (19, 53), guinea pig pancreatic lobules, without enzyme treatment to remove stromal support and extracellular adhesive factors, were incubated in 0.5 mM EGTA with gentle oscillation for up to 2 h. Abluminal junction strands were the first affected, migrating basally and becoming fragmented; one or more apical strands remained stable for at least 40 min and then also became disarranged and fragmented. The fragments and disarrayed strands were effective mechanical junctions, maintaining the cohesion of cells in lobules, and, upon restoration to medium containing Ca^{2+}, continuous zonulae occludentes were reassembled in 5–30 min. In their native connective-tissue stroma and three-dimensional tissue configuration, these cells apparently did not change shape conspicuously during EGTA treatment, and the micrographs revealed none of the tension effects on junction alignment or cell topography that we have observed in cultured mammary cells. Migration of junction strands may have been influenced by local tensions, but continuing oscillation did not prevent recovery after restoration of Ca^{2+}.

Ca^{2+} dependence of occluding junctions for both structure and function has been demonstrated in other systems. Martinez-Palomo et al. (27) recently showed that other divalent

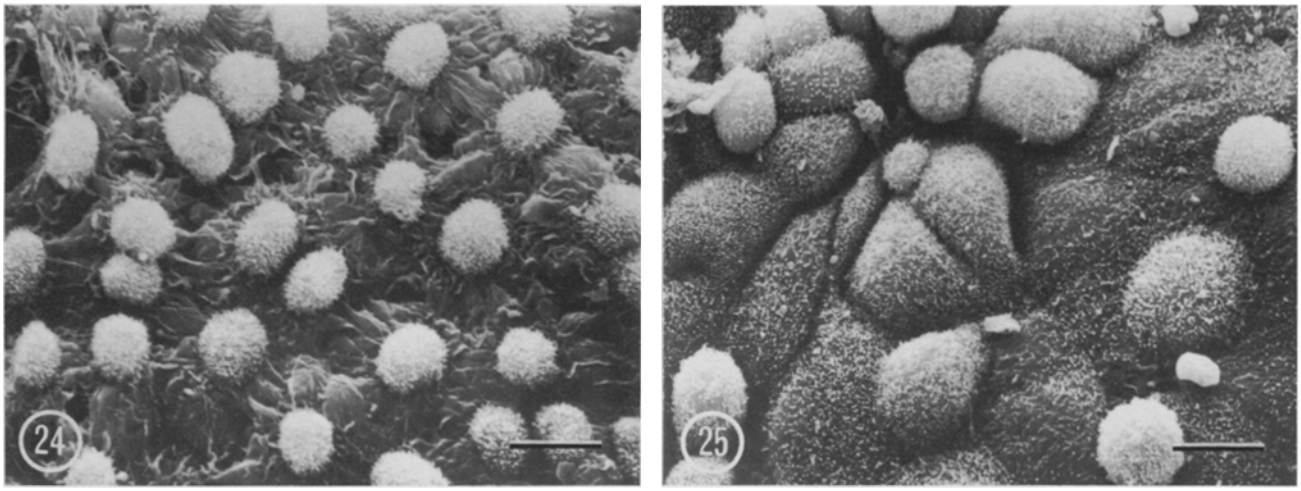

FIGURES 24 and 25 FIGURE 24 Culture on floating gel. Response of cells is more consistent on floating gels than on other substrates; all in this field show strong apical contraction with very densely crowded microvilli on the apical bulge. Filopodia are present in modest numbers but are relatively slack and inconspicuous. Peripheral membranes are ruffled but incompletely retracted. 1 mM EGTA at pH 8, 2.5 h. Bar, 5 μm. × 2,400. FIGURE 25 Floating gel culture, sister to that in Fig. 24 seeded at the same density and including the same number of cells in the field shown. After the same 2.5-h EGTA treatment, this culture was washed and incubated in culture medium for 4 h before being fixed for microscopy. Many cells are still rounded, but more are partly or completely spread, with few visible gaps between cell borders. Microvilli are almost uniformly distributed on flattened and moderately rounded cells, but border hedgerows have not reappeared. Bar, 5 μm. × 2,400.

cations (Mg^{2+}, Ba^{2+}) cannot replace Ca^{2+} in maintaining transepithelial electrical resistance in cultured MDCK cell monolayers mounted in Ussing-type chambers. 2.4 mM EGTA in Ca^{2+}-free medium caused a sharp drop in resistance to ~30% of the initial value within 10–15 min, followed by a slower decline. Zonulae occludentes remained morphologically intact during this drop; strand patterns were not altered beyond a small decrease in average number of continuous strands. Addition of the ionophore A23187 to medium containing Ca^{2+} caused the same loss of resistance as extracellular Ca^{2+} deprivation, suggesting that the latter condition may evoke release of Ca^{2+} from intracellular storage sites. Such an effect might also be instrumental in cytoskeletal contraction (54).

Effects of Other Agents

Increase in permeability of occluding junctions by exposure to hypertonic solutions has been demonstrated repeatedly. 240 mM urea applied to isolated toad urinary bladder made the junctions leaky and caused extensive blistering where intercellular space in compartments bounded by strands of the network swelled (55, 56). Similar effects were induced in other tissues by urea or various sugars or salts (57–59). Perfusion of mouse liver in situ with 0.5 mM disaccharides (60) caused plasmolysis and yielded examples of both gap and tight junctions that had split symmetrically. Freeze-fracture replicas showed typical strand networks in cell membranes separated by extracellular space from their partners. This is the only well documented instance of splitting, and it probably is not a mechanism for natural disassembly of junctions.

Proteases (12, 38, 61) can induce proliferation of strands, even in epithelial cells that previously had few or none. Phalloidin (62, 63), plant cytokinins (17, 63), and cAMP (63, 64) may induce increase in transepithelial resistance and abluminal extension of junction strands. Many other, unrelated, agents or conditions have been shown to cause disorderly displacement or proliferation of abluminal strands (see references in reference 35). Kachar and Pinto da Silva (35) described massive neoformation of strands in lateral membranes of prostate tissue explants after 5 min incubation at 37°C in any of several buffers or saline solutions. In view of the wide variety of stimuli that elicit this response, these authors concluded that it is a general reaction to nonspecific stressful conditions. We can now add that it is indicated in many tension-aligned junctions in low-density mammary cell cultures (29) and may occur in some EGTA-treated cells. If nothing else, strand proliferation would enhance intercellular cohesion. The reported stimuli apparently have no other feature in common than that they are all departures from prevailing normal conditions, making it appear likely that the phenomenon occurs in response to natural mild traumata in vivo, and could have protective value.

Cytoskeleton and Occluding Junctions

The hypothesis that control of occluding junction structure and function is mediated by the cytoskeleton is based largely on voluminous data demonstrating linkage of plasma membrane proteins to cortical actin-containing filaments (65–69). Evidence of association of cytoskeletal elements with the zonula occludens comes from electron microscopy of thin sections of intestinal brush border (70). Phalloidin, which stimulates actin polymerization, induced strand proliferation and enhanced transepithelial resistance in *Necturus* gallbladder (62, 63). Cytochalasin B at 0.1–0.6 μg/ml also increased resistance, but higher concentrations reduced it in the gallbladder (63) and in MDCK monolayers (49); 20 μg/ml inhibited junction formation in a colon cell line (71), but a similar concentration did not affect maintenance, EGTA-induced fragmentation, or reassembly of occluding junctions in pancreatic lobules (53). High-resolution immunoelectron microscopy was used by Geiger (68) to examine the distribution of vinculin and α-actinin, two of the proteins thought to be involved in linkage of actin filaments to plasma membranes, in intestinal brush border. In the area of the junctional complex, vinculin was confined to the immediate vicinity of the zonula adhaerens membrane; α-actinin was also abundant around the zonula adhaerens but somewhat farther from the membrane surface, and some label was present near the zonula occludens.

In our experiments, centripetal contraction occurred in a zone presumably corresponding to the zonula adhaerens. The effect on the zonula occludens could have been mediated by linkage of contractile filaments to junction strands or less directly by tensions in the cortical cytoskeletal meshwork and a contiguous layer of membrane-associated proteins (72). Both thin-section electron microscopy and the observed activity of peripheral membranes indicate that cytoskeletal elements remain associated with these membranes throughout Ca^{2+}-dependent junction disassembly. Further study of the identity and distribution of cytoskeletal components is in progress.

CONCLUSIONS

Much more is known about the electrophysiology of occluding junction permeability (10) than about the structure that provides the variable permeability barrier. It is evident that maintenance both of electrical resistance and of morphological integrity of the occluding junction requires an (unknown) appropriate level of Ca^{2+} bound to or in the vicinity of the plasma membrane. The process of disassembly experimentally induced by withdrawal of extracellular Ca^{2+} should reflect some aspects of normal regulation. The available evidence now indicates that major factors are local cytoskeletal influence on strand position, variation in membrane viscosity, and mechanical stress.

We suggest that mechanical forces normally encountered in vivo can be important in the stability and modulation of occluding junction structure. In cell culture, tension alone can cause realignment of strands (29), and when accompanied by decrease in membrane viscosity can reduce junction belts to widely separated fragments. In vivo, epithelial cell sheets are supported by fibrous stroma and typically fastened together by junctional complexes wherein zonulae and maculae adhaerentes help to protect the all-important zonula occludens from drastic effects of inherent or imposed tension. But strand alignment may in at least some cases be determined by, as well as adapted to, normal mechanical stress. This is an appealing possibility in the case of junctions subjected to periodic stretching (9, 73), which often display a pattern of undulating strands predominantly paralleling the apical border. In cases of abnormal stress, realignment of strands parallel to the axis of tension could reduce the probability of extensive tearing.

We are grateful to the Electron Microscope Laboratory, University of California, Berkeley, for the use of its freeze-fracture and scanning electron microscopy facilities, to John Underhill and Lionel Thomas for assistance with photographic procedures, and to Susie Castillo for expert secretarial assistance.

Our work was supported by National Institutes of Health grants GM26230 and CA05388, Department of Health and Human Services.

Received for publication 17 May 1982, and in revised form 3 November 1982.

REFERENCES

1. Revel, J. P., P. Yip, and L. L. Chang. 1973. Cell junctions in the early chick embryo—a freeze etch study. *Dev. Biol.* 35:302–317.
2. Reeves, W., J. P. Caulfield, and M. G. Farquhar. 1978. Differentiation of epithelial foot processes and filtration slits. Sequential appearance of occluding junctions, epithelial polyanion, and slit membranes in developing glomeruli. *Lab. Invest.* 39:90–100.
3. Decker, R. S. 1981. Disassembly of the zonula occludens during amphibian neurulation. *Dev. Biol.* 81: 12–22.
4. Friend, D. S., and N. B. Gilula. 1972. Variations in tight and gap junctions in mammalian tissues. *J. Cell Biol.* 53:758–776.
5. Claude, P. 1978. Morphological factors influencing transepithelial permeability: a model for the resistance of the zonula occludens. *J. Membr. Biol.* 39:219–232.
6. Ernst, S. A., W. C. Dodson, and K. J. Karnaky, Jr. 1980. Structural diversity of occluding junctions in the low-resistance chloride-secreting opercular epithelium of seawater-adapted killifish (*Fundulus heteroclitus*). *J. Cell Biol.* 87: 488–497.
7. Schneeberger, E. E. 1980. Heterogeneity of tight junction morphology in extrapulmonary and intrapulmonary airways of the rat. *Anat. Rec.* 198:193–208.
8. Tice, L. W., R. L. Carter, and M. B. Cahill. 1979. Changes in tight junctions of rat intestinal crypt cells associated with changes in their mitotic activity. *Tissue & Cell.* 11:293–316.
9. Pitelka, D. R., S. T. Hamamoto, J. G. Duafala, and M. K. Nemanic. 1973. Cell contacts in the mouse mammary gland. I. Normal gland in postnatal development and the secretory cycle. *J. Cell Biol.* 56: 797–818.
10. Erlij, D., and A. Martinez-Palomo. 1978. Role of tight junctions in epithelial function. *In* Membrane Transport in Biology. G. Giebisch, D. C. Tosteson and H. H. Ussing, editors. Springer-Verlag, Berlin. 3:27–53.
11. Bullivant, S. 1981. Possible relationships between tight junction structure and function. *In* Epithelial Ion and Water Transport. A. D. C. Macknight and J. P. Leader, editors. Raven Press, New York. 265–275.
12. Orci, L., M. Amherdt, J. C. Henquin, A. E. Lambert, R. H. Unger, and A. E. Renold. 1973. Pronase effect on pancreatic beta cell secretion and morphology. *Science* (*Wash. DC*) 180:647–649.
13. Erlij, D., and A. Martinez-Palomo. 1972. Opening of tight junctions by hypertonic urea solutions. *J. Membr. Biol.* 9:229–240.
14. Brightman, M. W., M. Hori, S. L. Rapoport, T. S. Reese, and E. Westergaard. 1973. Osmotic opening of tight junctions in the cerebral endothelium. *J. Comp. Neurol.* 152:317–325.
15. Rhodes, R. S., and M. J. Karnovsky. 1971. Loss of macromolecular barrier function associated with surgical trauma to the intestine. *Lab. Invest.* 25:220–229.
16. Carson, J. L., A. M. Collier, and S. S. Hu. 1980. Ultrastructural studies of hamster tracheal epithelium *in vivo* and *in vitro*. *J. Ultrastruct. Res.* 70:70–81.
17. Bentzel, C. J., B. Hainau, A. Edelman, T. Anagnostopoulos, and E. L. Benedetti. 1976. Effect of plant cytokinins on microfilaments and tight junction permeability. *Nature* (*Lond.*). 264:666–668.
18. Sedar, A. W., and J. G. Forte. 1964. Effects of calcium depletion on the junctional complex between oxyntic cells of gastric glands. *J. Cell Biol.* 22:173–188.
19. Galli, P., A. Brenna, P. de Camilli, and J. Meldolesi. 1976. Extracellular calcium and the organization of tight junctions in pancreatic acinar cells. *Exp. Cell Res.* 99:178–183.
20. Leighton, J., F. Brada, L. W. Estes, and G. Justh. 1969. Secretory activity and oncogenicity of a cell line (MDCK) derived from canine kidney. *Science* (*Wash. DC*). 163:472–473.
21. Pickett, P. B., D. R. Pitelka, S. T. Hamamoto, and D. S. Misfeldt. 1975. Occluding junctions and cell behavior in primary cultures of normal and neoplastic mammary gland cells. *J. Cell Biol.* 66:316–332.
22. Misfeldt, D. S., S. T. Hamamoto, and D. R. Pitelka. 1976. Transepithelial transport in cell culture. *Proc. Natl. Acad. Sci. USA* 73:1212–1216.
23. Rabito, C. A., R. Tchao, J. Valentich, and J. Leighton. 1978. Distribution and characteristics of the occluding junctions in a monolayer of a cell line (MDCK) derived from canine kidney. *J. Membr. Biol.* 43:351–363.
24. Bisbee, C. A., T. E. Machen, and H. A. Bern. 1979. Mouse mammary epithelial cells on floating collagen gels: transepithelial ion transport and effects of prolactin. *Proc. Natl. Acad. Sci. USA* 76:536–540.
25. Handler, J. S., R. E. Steele, M. K. Sahib, J. B. Wade, A. S. Preston, N. L. Lawson, and J. P. Johnson. 1979. Toad urinary bladder epithelial cells in culture: maintenance of epithelial structure, sodium transport, and response to hormones. *Proc. Natl. Acad. Sci. USA* 76:4151–4153.
26. Cereijido, M., E. S. Robbins, W. J. Dolan, C. A. Rotunno, and D. P. Sabatini. 1978. Polarized monolayers formed by epithelial cells on a permeable and translucent support. *J. Cell Biol.* 77:853–880.
27. Martinez-Palomo, A., I. Meza, G. Beaty, and M. Cereijido. 1980. Experimental modulation of occluding junctions in a cultured transporting epithelium. *J. Cell Biol.* 87:736–745.
28. Pitelka, D. R., and S. T. Hamamoto. 1977. Calcium-chelation-induced disruption of occluding junctions by cultured mammary epithelial cells. *J. Cell Biol.* 75:69a. (Abstr.)
29. Pitelka, D. R., AND B. N. Taggart. 1983. Mechanical tension induces lateral movement of intramembrane components of the tight junction. Studies on mouse mammary cells in culture. *J. Cell Biol.* 96:606–612.
30. White, M. T., A. S. L. Hu, S. T. Hamamoto, and S. Nandi. 1978. In vitro analysis of proliferating epithelial cell populations from the mouse mammary gland: fibroblast-free growth and serial passage. *In Vitro.* 14:271–281.
31. Richardson, K. C., L. Jarett, and E. H. Fincke. 1960. Embedding in epoxy resins for ultrathin sectioning in electron microscopy. *Stain Technology.* 35:313–323.
32. Cohen-Solal, L., M. Cohen-Solal, and M. J. Glimcher. 1979. Identification of γ-glutamyl phosphate in the α-2 chains of chicken bone collagen. *Proc. Natl. Acad. Sci. USA* 76:4327–4330.
33. Teng, H.-H., and D. B. Rifkin. 1979. Fibronectin from chicken embryo fibroblasts contains covalently bound phosphate. *J. Cell Biol.* 80:784–791.
34. Emerman, J. T., S. J. Burwen, and D. R. Pitelka. 1979. Substrate properties influencing ultrastructural differentiation of mammary epithelial cells in culture. *Tissue & Cell* 11:109–119.
35. Kachar, B., and P. Pinto da Silva. 1981. Rapid massive assembly of tight junction strands. *Science* (*Wash. DC*) 213:541–544.
36. Staehelin, L. A. 1973. Further observations on the fine structure of freeze-cleaved tight junctions. *J. Cell Sci.* 13:763–786.
37. Staehelin, L. A. 1974. Structure and function of intercellular junctions. *Int. Rev. Cytol.* 39:191–283.
38. Polak-Charcon, S., J. Shoham, and Y. Ben-Shaul. 1978. Junction formation in trypsinized cells of human adenocarcinoma cell line. *Exp. Cell Res.* 116:1–13.
39. Polak-Charcon, S., and Y. Ben-Shaul. 1979. Degradation of tight junctions in HT29, a human colon adenocarcinoma cell line. *J. Cell Sci.* 35:393–402.
40. Porvaznik, M. 1979. Tight junction disruption and recovery after sublethal irradiation. *Radiat. Res.* 78:233–250.
41. Gordon, L. M., R. D. Sauerheber, and J. A. Esgate. 1978. Spin label studies on rat liver and heart plasma membranes: effects of temperature, calcium, and lanthanum on membrane fluidity. *J. Supramol. Struct.* 9:299–326.
42. Campisi, J., and C. J. Scandella. 1980. Calcium-induced decrease in membrane fluidity of sea urchin egg cortex after fertilization. *Nature* (*Lond.*). 286:185–186.
43. Talmon, A., and Y. Ben-Shaul. 1979. Tight junctions of dissociated and reaggregated embryonic lung cells. *Cell Differ.* 8:437–450.
44. Lane, N. J., and L. S. Swales. 1980. Dispersal of junctional particles, not internalization, during the in vivo disappearance of gap junctions. *Cell.* 19:579–586.
45. Britch, M., and T. D. Allen. 1980. The modulation of cellular contractility and adhesion by trypsin and EGTA. *Exp. Cell Res.* 125:221–231.
46. Rosen, J. J., and L. A. Culp. 1977. Morphology and cellular origins of substrate-attached material from mouse fibroblasts. *Exp. Cell Res.* 107:139–149.
47. Glässer, D., W. Rattke, and M. Iwig. 1979. Bovine lens epithelium: a suitable model for studying growth control mechanisms. *Exp. Cell Res.* 122:281–292.
48. Batten, B. E., and E. Anderson. 1981. Effects of Ca^{2+} and Mg^{2+} deprivation on cell shape in cultured ovarian granulosa cells. *Am. J. Anat.* 161:101–114.
49. Meza, I., G. Ibarra, M. Sabanero, A. Martinez-Palomo, and M. Cereijido. 1980. Occluding junctions and cytoskeletal components in a cultured transporting epithelium. *J. Cell Biol.* 87:746–754.
50. Berry, M. N., and D. S. Friend. 1969. High-yield preparation of isolated rat liver parenchymal cells. A biochemical and fine structural study. *J. Cell Biol.* 43:506–520.
51. Amsterdam, A., and J. D. Jamieson. 1974. Studies on dispersed pancreatic exocrine cells. I. Dissociation technique and morphologic characteristics of separated cells. *J. Cell Biol.* 63:1037–1056.
52. Dermietzel, R., K. Meller, W. Tetzloff, and M. Waelsch. 1977. In vivo and in vitro formation of the junctional complex in choroid epithelium. A freeze-etching study. *Cell Tissue Res.* 181:427–441.
53. Meldolesi, J., G. Castiglioni, R. Parma, N. Nassivera, and P. de Camilli. 1978. Ca^{++}-dependent disassembly and reassembly of occluding junctions in guinea pig pancreatic acinar cells. *J. Cell Biol.* 79:156–172.
54. Lee, H. C., and N. Auersperg. 1980. Calcium in epithelial cell contraction. *J. Cell Biol.* 85:325–336.
55. Wade, J. B., and M. J. Karnovsky. 1974. Fracture faces of osmotically disrupted zonulae occludentes. *J. Cell Biol.* 62:344–350.
56. Wade, J. B., J. P. Revel, and V. A. DiScala. 1973. Effect of osmotic gradients on intercellular junctions of the toad bladder. *Am. J. Physiol.* 224:407–415.
57. Rapoport, S. I., and H. K. Thompson. 1973. Osmotic opening of the blood-brain barrier in the monkey without associated neurological deficits. *Science* (*Wash. DC*). 180:971.
58. Bouchaud, B., and D. Bouvier. 1978. Fine structure of tight junctions between rat choroidal cells after osmotic opening induced by urea and sucrose. *Tissue & Cell.* 10:331–342.
59. Cooper, M., S. Teichberg, and F. Lifshitz. 1978. Alterations in rat jejunal permeability to a macromolecular tracer during a hyperosmotic load. *Lab. Invest.* 38:447–454.
60. Goodenough, D. A., and N. B. Gilula. 1974. The splitting of hepatocyte gap junctions and zonulae occludentes with hypertonic disaccharides. *J. Cell Biol.* 61:575–590.
61. Shimono, M., and F. Clementi. 1977. Intercellular junctions of oral epithelium. II. Ultrastructural changes in rat buccal epithelium induced by trypsin digestion. *J. Ultrastruct. Res.* 59:101–112.
62. Montesano, R., G. Gabbiani, A. Perrelet, and L. Orci. 1976. *In vivo* induction of tight junction proliferation in rat liver. *J. Cell Biol.* 68:793–798.
63. Bentzel, C. J., B. Hainau, S. Ho, S. W. Hui, A. Edelman, T. Anagnostopoulos, and E. L. Benedetti. 1980. Cytoplasmic regulation of tight-junction permeability: effect of plant cytokinins. *Am. J. Physiol.* 239:C75–C89.
64. Duffey, M. E., B. Hainau, S. Ho, and C. J. Bentzel. 1981. Regulation of epithelial tight junction permeability by cyclic AMP. *Nature* (*Lond.*). 294:451–453.
65. Nicolson, G. L. 1976. Transmembrane control of the receptors on normal and tumor cells. I. Cytoplasmic influence over cell surface components. *Biochim. Biophys. Acta.* 457:57–108.
66. Singer, I. I. 1979. The fibronexus: a transmembrane association of fibronectin-containing fibers and bundles of 5 nm microfilaments in hamster and human fibroblasts. *Cell* 16:675–685.
67. Elson, E. L., and J. A. Reidler. 1979. Analysis of cell surface interactions by measurements of lateral mobility. *J. Supramolec. Struct.* 12:481–489.
68. Geiger, B., A. H. Dutton, K. T. Tokuhasu, and S. J. Singer. 1981. Immunoelectron microscope studies of membrane-microfilament interactions: distributions of α-actinin, tropomyosin, and vinculin in intestinal epithelial brush border and chicken gizzard smooth muscle cells. *J. Cell Biol.* 91:614–628.
69. Koppell, D. E., M. P. Sheetz, and M. Schindler. 1981. Matrix control of protein diffusion in biological membranes. *Proc. Natl. Acad. Sci. USA* 78:3576–3580.
70. Hull, B. E., and L. A. Staehelin. 1979. The terminal web: a reevaluation of its structure and function. *J. Cell Biol.* 81:67–82.
71. Polak-Charcon, S., and Y. Ben-Shaul. 1978. Tight junction assembly in human adenocarcinoma cell line: relations to cytoskeletal elements. 9th International Congress of Electron Microscopy, Toronto, 1978. 2:334–335.
72. Ben-Ze'ev, A., A. Duerr, F. Salamon, and S. Penman. 1979. The outer boundary of the cytoskeleton, a lamina derived from plasma membrane protein. *Cell.* 17:859–866.
73. Hull, B. E., and L. A. Staehelin. 1976. Functional significance of the variations in the geometrical organization of tight junction networks. *J. Cell Biol.* 68:688–704.